

Supplementary file for ‘Geology, Petrology and O and H isotope geochemistry of remarkably ^{18}O depleted Paleoproterozoic rocks of the Belomorian Belt, Karelia, Russia, attributed to the Slushball Earth’ by Bindeman I.N., Serebryakov N.S.

Methods

Oxygen isotope analyses of plagioclase, ruby corundum, kyanite, biotite, amphibole, garnet, zircon, monazite, and rutile relied on 0.5-2 mg aliquots and were performed at the University of Oregon stable isotope lab using CO_2 -laser fluorination (Bindeman, 2008). We concentrated on single grain analyses where size permitted (shown as Pl-1, Gt-1 etc in **Table A1** below). Samples were heated up by a NewWave 35Watts laser in the presence of purified BrF_5 reagent to liberate oxygen. The gas generated in the laser chamber was purified through a series of cryogenic traps held at liquid nitrogen temperature, and a mercury diffusion pump to remove traces of fluorine gas. Oxygen was converted to CO_2 gas in a small platinum-graphite converter, the yields were measured, and then CO_2 gas was analyzed on a MAT 253 mass spectrometer in a dual inlet mode. Four to seven Gore Mt. Garnet standard ($\delta^{18}\text{O} = 5.75\text{‰}$) were analyzed together with the unknowns during each of seven analytical sessions. Day-to-day $\delta^{18}\text{O}$ variability of standards ranged from being 0.1 to 0.35‰ lighter than their reference values and the measurements of unknowns were adjusted to correct for day-to-day variability. The precision on standards is better than 0.1‰ 1 st dev on average.

Because samples were significantly lighter in $\delta^{18}\text{O}$ than our standard (and no standard as negative as the reported values exist to our knowledge), one might worry about analytical offsets related to the memory effects. However, garnet standard run after -20‰ unknown did not display downward shift by more than -0.1‰ as compared to normal- $\delta^{18}\text{O}$ samples run in different data blocks of the same analytical session; we therefore accept that memory effects on the order of 0.1‰ could have affected the measured values but we choose not to apply any special corrections other than those outlined above, given the remarkably large $\delta^{18}\text{O}$ range found. Mass spectrometry analyses of isotopically negative samples vs a standard gas should not result in unexpected deltas because calculation of deltas is done using raw ratios.

We additionally performed oxygen isotope measurements for 2 samples using O_2 gas as analute without converting it to CO_2 in order to check for mass-independent ^{17}O anomaly. This anomaly could signify potential extraterrestrial (e.g. cometary) origin of ultradepleted $\delta^{18}\text{O}$ Karelian gneisses, or Archean mass-independent effects due to atmospheric photolysis. The O_2 measurements are routinely performed at the University of Oregon Stable Isotope lab to characterize mass independent ^{17}O excesses in terrestrial (Martin and Bindeman 2009) and extraterrestrial materials such as HED meteorites (Ruzicka et al. in prep) and we have good calibration procedures for $\Delta^{17}\text{O}$. However two measurements yielded $\Delta^{17}\text{O} = 0\text{‰}$ thus denying the possibility of extraterrestrial or atmospheric photolytic origin.

Hydrogen isotope measurements relied on 1-2 mg of individual and bulk biotite and amphibole crystals and were performed in a continuous flow mode using UHP He carrier gas and TC/EA furnace with glassy carbon (improved after Sharp et al. 2001). We employed three out of four solid standards in three analytical sessions (NBS30 biotite, $\delta\text{D} = -66\text{‰}$, Water Canyon biotite, $\delta\text{D} = -106\text{‰}$, Butte Montana BUD biotite $\delta\text{D} = -161.8\text{‰}$, and RUH2 muscovite, $\delta\text{D} = -98.2\text{‰}$) spanning the range of 95‰ and overlapping with the ranges of the unknowns. We applied three point calibration using offsets between obtained δD values and the quoted values for mica standards run during each analytical session. Instrumental mass fractionation offset were typically between 20 and 30‰ and the magnitude of offset differed by less than 10‰ in lighter vs. heavy D/H ends. Based on the repeat values of standards, the 1 st deviation ranged in the $\pm 2\text{-}3\text{‰}$ range. Furthermore, in the beginning of each analytical

session we applied H3 factor at different pressure of the carrier gas to correct for different peak heights. Water concentrations were determined by mass H2 peak integration and the uncertainty is estimated to be ± 0.05 wt% based on standards. As biotite and amphibole have ~ 4 - 4.5 and ~ 2 wt% H2O respectively, the amount of alteration by chlorite (a phase with ~ 10 wt% H2O) can be estimated based on water concentration (high-H2O samples).

Carbon and oxygen isotopic measurement on a single magnesite sample were performed using phosphoric acid digestion at 70°C on GasBench device, and using 8.7 ‰ for fractionation factor for $\delta^{18}\text{O}$ between released CO_2 and the analyzed carbonate. Choice of different fractionation factors change the estimate by less than 1 permil (Zheng et al. 1996).

Table 1 Oxygen and hydrogen isotope geochemistry of uniquely low- $\delta^{18}\text{O}$ metamorphic rocks from the Belomorian Belt of Karelia

Sample	mineral	$\delta^{18}\text{O}$	$\delta^{18}\text{O}_{\text{wr}}$	Rock type	Longitude	Latitude
		min, ‰	calc, ‰			
<i>Khitostrov (see map on Fig. 2)</i>						
X5-1	Bi	-11.59	-9.0	Ms-Bi-Pl rock		
X5-1	Pl	-8.4				
X14a	Pl	-20.01	-21.1	migmatized Gt gabbro-amphibolite	34411	4090
X14a	Cam	-22.27				
X15-1	Pl	-16.63	-17.4	migmatized Gt gabbro amphibolite	34412	4044
X15-1	Cam	-18.27				
X15-3	Pl	-16.36	-17.2	migmatized Gt gabbro amphibolite	34412	4044
X15-3	Cam	-17.98				
X12a	Pl	-12.59	-13.6	Gt-Bi gneiss	34411	4090
X12a	Bi	-15.45				
X112	Pl-1	-8.80	-8.8	Plagioclase		
X174	Qz	-6.64	-7.5	Ms-Bi-gneiss		
X174	Pl-1	-8.05				
X245	Pl	6.48	5.7	metamorphozed Fe-gabbro		
X245	Cam	4.96				
X246	Pl	6.66	5.7	metamorphozed Fe-gabbro		
X246	Cam	4.72				
X305b	Pl	-15.88	-18.3	Ky-Gt-Bi-Pl±Qz rocks		
X305b	Gt	-18.79				
X310	Pl-1	-14.49	-17.8	Ky-Gt-Bi-Pl±Qz rocks		
X310	Gt-1	-18.3				
X335	Pl	-15.27	-19.6	St-Gt-Bi-Pl rocks with		
X335	Gt	-20.15		St-Pl pseudomorphs over Ky		
X401	Qz-1	4.80	2.8	Qz-Pl-Bi pegmatite		
X401	Pl	3.15				
X402	Qz-1	-13.10	-15.1	Bi-Gt gneiss	34158	4171
X402	Pl-1	-14.65				
X403	Gt	-1.97	-2.0	migmatized Gt-amphibolite	34148	4345
X403	Gt	-0.88	-0.9	migmatized Gt-amphibolite	34148	4345
X404	Qz-1	9.41	7.4	Gt-Bi gneiss	34093	4409
X405	Cam	-1.5				
X405	Gt	-2.94	-2.9	migmatized Gt-amphibolite	34097	4420
X406	Qz-1	9.77	7.8	Gt-Bi gneiss	34134	4732
X407	Gt	1.78	0.2	Gt-Bi gneiss	34142	4827
X407	Pl	-0.90				
X408	Pl	8.86	8.9	Gt-Bi gneiss	34217	5191
X409	Pl-1	11.66	11.7	Gt-Bi gneiss	34133	5400
X410a	Gt	4.85	4.9	metamorphozed Fe-gabbro	34099	5269
X410b	Qz-1	8.11	6.1	Pl-Qz vein in metamorphozed Fe-gabbro	34099	5269
X411	Gt	7.09	7.6	Ky-Gt-Bi gneiss	34254	5149
X412	Qz	9.64	7.6	Gt-Bi-Ky gneiss	34283	4937
X413	Qz	3.43	1.7	Bi-gneiss, leucocratic	34312	4716
X413	Qz-1	3.96				
X414	Qz	-1.48	-3.5	Gt-Bi gneiss leucocratic	34310	4470
X415	Qz	10.49	8.5	Gt-Bi gneiss	34361	4249
X416	Gt	6.84	6.8	Gt-Bi gneiss	34359	4244
X417	Gt	-8.88	-8.9	migmatized Gt-amphibolite		
X418	Gt	-7.70	-7.7	migmatized Gt-amphibolite		
X419	Gt	-15.97	-16.0	migmatized Gt-amphibolite		
X420	Gt	-15.75	-15.8	migmatized Gt-amphibolite		
X421	Gt	-16.74	-16.7	St-Gt-Bi-Pl rocks with St-Pl pseudomorphs over Ky	34343	4224
X422	Gt	-17.02	-17.0	St-Gt-Bi-Pl rocks with St-Pl pseudomorphs over Ky		
X423	Pl-1	-22.85		Crn-St-Gt-Bi-Cam-Pl rocks with Crn-St-Pl pseudomorphs over Ky	34377	4003
X423	Gt	-24.94	-24.4	Crn-St-Gt-Bi-Cam-Pl rocks with Crn-St-Pl pseudomorphs over Ky	34377	4003
X424	Gt	-25.38	-25.4	Crn-St-Gt-Bi-Cam-Pl rocks with coarse grained Crn	34333	3979
X424	Gt-1	-26.54	-26.5			
X424	Cam	-25.48	-26.0			
X424	Pl	-23.94				
X424	Pl-1	-22.59				
X425	Pl	-23.49				
X425	Gt-1	-26.17	-26.2	Crn-St-Gt-Bi-Prg-Pl rocks with coarse grained Crn	34332	3977
X425	Gt, 2 Xtls	-26.94	-26.9			
X425	Crn-1	-25.96	-26.0	Crn-St-Gt-Bi-Prg-Pl rocks with coarse grained Crn	34332	3977
X425	Cam-1	-24.46	-24.5			
X426	Pl-1	-23.28				
X426	Pl	-23.56				
X426	Gt	-25.68	-25.7			
X426	Cam	-25.28	-25.8	Crn-St-Gt-Bi-Prg-Pl rocks with coarse grained Crn	34333	3979
X426	Crn	-23.69	-23.7	Crn-St-Gt-Bi-Prg-Pl rocks with coarse grained Crn	34333	3979

Sample	mineral	$\delta^{18}\text{O}$	$\delta^{18}\text{O}_{\text{wr}}$	H ₂ O	δD	Rock type	Longit	Latitude	
		min, ‰	calc, ‰	wt% ‰	wt% ‰				
X427	Pl	-22.14				Crn-St-Gt-Bi-Prg-Pl rocks with coarse grained Crn	34324	3925	
X427	Gt	-24.83	-24.8			Crn-St-Gt-Bi-Prg-Pl rocks with coarse grained Crn	34324	3925	
X428	Qz-1	-2.64	-4.6			Qz-Mus plagioclase	34295	3886	
X429	Qz	10.37	8.4			Bi gneiss	34232	2098	
X430a	Gt	7.31	7.8			Gt-Bi gneiss melanosome	34201	2200	
X430b	Qz	10.20	8.2			Gt-Bi gneiss leucosome	34201	2200	
X431	Gt-1	7.16	7.7			Ky-Gt-Bi-gneiss	34139	2404	
X432	Gt-1	7.23	7.7			Gt-Bi gneiss	34285	2565	
X433	Gt	5.67	5.7			Gt gabbro-amphibolite	34285	2565	
X434	Gt-1	7.47	8.0			Ky-Gt-Bi gneiss	34476	4086	
X435	Qz-1	10.35	8.4			Ky-Gt-Bi gneiss leucosome	34492	3994	
X436	Qz	-8.71	-10.7			Gt-Bi gneiss	34449	3737	
X436	Pl-1	-12.9							
X437	Pl-1	-13.2							
X437	Gt	-13.50	-13.0			leucocratic Pl-Cam-Bi-Gt-St-Crn rocks with coarse grained Crn	34419	3779	
X438	Pl-1	-16.45	-18.5			St-Gt-Bi-Pl rocks with St-Pl pseudomorphs over Ky	34414	4021	
X439	Gt	-24.77	-24.8			leucocratic Pl-Cam-Bi-Gt-St-Crn rocks with coarse grained Crn	34347	3888	
X440	Gt-1	-1.84	-1.3			Gt-Bi gneiss	34410	4092	
X441	Pl	4.39	4.4			Gt-Bi gneiss	34409	4160	
X442	Gt	-22.16	-21.7			Crn-St-Gt-Bi-Prg-Pl rocks with coarse grained Crn	34410	3990	
X443	Gt	-23.76	-23.3			Crn-St-Gt-Bi-Prg-Pl rocks with coarse grained Crn	34410	3984	
X444	Gt	-22.35	-21.8			Crn-St-Gt-Bi-Prg-Pl rocks with coarse grained Crn	34406	3989	
X445	Gt	-23.02	-23.0			monomineralic Cam rocks	34406	3989	
X446	Gt	-24.08	-24.1			Crn-St-Gt-Bi-Prg-Pl rocks with coarse grained Crn	34407	3979	
X447	Gt	-24.05	-24.1			Crn-St-Gt-Bi-Prg-Pl rocks with coarse grained Crn	34406	3959	
X448	Crn	-18.65	-18.6			Pl-Bi-Gt-St-Crn rocks with coarse grained Crn	34411	3940	
X449	Gt	-20.22	-20.2			Crn-Ky-St-Gt-Bi-Pl rocks	34413	3933	
X450	Gt-1	-10.69	-10.7			Ky-Gt-Bi gneiss	34280	3767	
X451	Qz	-3.46	-5.5			Gt gabbro-amphibolite	34246	3584	
X451	Cam-1	-7.32							
Area around Khitostrov									
X452	Gt	6.97	7.5			Ky-Gt-Bi gneiss Chupa gneiss Malinovaya Varaka mine	30914	20674	
X453	Gt	7.40	7.9			Ky-Gt-Bi gneiss leucosome Chupa gneiss Malinovaya Varaka mine	30914	20674	
X454	Gt-1	6.16	6.7			Gt-Qz-Pl pegmatite 1.9 , Malinovaya Varaka mine	30914	20674	
X455	Gt-1	8.53	9.0			Ky-Gt-Bi gneiss Chupa gneiss quarry lake Dolgoye	30943	7912	
X456	Qz	10.49	8.5			2.6 Ga granite, quarry lake Dolgoye	30943	7912	
X458	Gt	5.51	5.5			gabbro-norite, 2.4 Ga 3 km from Khitostrov, U Pulongskoye lake	30146	4756	
H107	Qz	8.94	6.9			1.9 Ga pegmatite from Khetolambino quarry	35217	3701	
Varatskoye see map on Fig. 4									
meta morphic rocks developed over gabbro									
V51	Pl	-14.07				Cam schist, monomineralic with minor Pl, coarse-grained	66.22	33.125	
V51	Cam-1	-15.92	-15.7	3.03	-226.8				
V52	Cam-1	-15.70	-15.7	2.8	-224.3	Cam-Oam rock, coarse-grained	66.22	33.125	
V49	Gt -1	-17.37				Gt-Cam rock with Ky substituted by St-Pl			
V49	Cam-1	-16.08	-16.5	4.14	-218.7		66.22	33.125	
V81a	Cam-1	-18.54	-18.4	3.71	-228.1	Crn-Cam rock, coarse grained	66.22	33.125	
V81a	Crn-1	-17.27							
V53	Gt-1, megacrysts	-19.18	-19.2			Gt substituted by Cam-Spinel-Ged-Chl			
V53	Ged-1	-8.57		2.7	-180.1	retrogressed Ged	66.22	33.125	
meta morphic rocks developed over Ky-gneiss									
V40	Gt-1	-18.77	-18.3			Ky-Gt-Bi-Pl rock			
V40	Pl-1	-13.33							
V41	Cam-1	-19.08	-18.4	3.98	-233.0	St-Gt-Bi-Cam-Pl rocks with St-Pl pseudomorphs over Ky	66.22	33.125	
V41	Gt -1	-18.76							
V45	Pl-1	-17.82				Crn-St-Cam-Pl rock, with coarse grained	66.22	33.125	
V45	Crn-1	-19.20	-18.9			Crn and Crn-St-Pl substituting Ky			
V45	Cam	-19.54		3.55	-233.4				
V100	Opx	5.34	5.8			Cpx-Pl-Opx gabbro norite	66.2	33.091	
V101	Pl-1	-17.62	-17.6			Ky-Gt-Bi gneiss	66.23	33.126	
V101	Gt-1	-16.16							
V102	Qz-1	10.44	8.4			Ky-Gt-Bi gneiss	66.23	33.133	
V102	Gt	8.14	8.6						
V103	Qz-1	11.22	9.2			Ky-Gt-Bi gneiss	66.22	33.136	
V103	Gt-1	8.60	9.1						
V104	Cam-1	-2.57	-2.2			Ky-Gt-Qz-Bi-Cam-Pl rock	66.23	33.127	
V104	Gt-1	-1.75	-1.3						

Sample	mineral	$\delta^{18}\text{O}$ min, ‰	$\delta^{18}\text{O}$,wr calc, ‰	H ₂ O wt%	δD ‰	Rock type	Longitude	Latitude
--------	---------	---------------------------------	--------------------------------------	-------------------------	-----------------------	-----------	-----------	----------

Mt Dyadina, see map on Fig. 3

metamorphic rocks developed over gabbro-norite close to its contact with gneiss

DG-70	Pl-1	7.07	6.0			Cpx-Pl-Opx±Gt±Bi gabbro-norite		
DG-70	Px-1	5.68				weakly metamorphosed	66.44	32.615
DG-16	Cam-1	-0.07	-0.1	2.86	-87.1	Cam-Gt rock, coarse-grained	66.44	32.616
DG-16	Pl	3.56				secondary Pl		
DG-16	Qz	7.54				secondary Qz		
DG-17	Ky-1	0.67	0.9			Ky-Cam-Oam rock, medium-grained		
DG-17	Oam			3.3	-88.1			
DG17	Cam	0.52		2.53	-86.7			
DG113	Ged	1.73				Ged-Ky rock, coarse-grained	66.44	32.616
DG-113	Ky-1	0.4	0.7					
DG-121	Oam-1	3.31	3.3	3.32	-81.4	Ged-Spr-Mgn-Gt rock, giant Gt		
DG-121	Sapphyrine	2.39						
DG-121	Magnesite	10.37				$\delta^{13}\text{C} = -7.4$ ‰, secondary		
DG-117	Gt-1	-0.58	-0.6			giant Gt megacryst		
DG-117i	Crn-1	0.49	1.3			inclusion of Cam-Crn in giant Gt		
DG-117i	Cam-1	2.12		3.05	-92.9			
DG-32	Gt-1	-0.50				Gt-Ant-Chl rock, coarse-grained, giant Gt		
DG-32	Cam-1	-0.49	-0.5				66.44	32.616
DG-25	Gt -1	-0.68				St-Gt-Cam rock, medium-grained	66.44	32.616
DG-25	Cam-1	-1.16	-1.0	3.44	-95.0			
DG64A	Cam-1	1.67	1.4	3.4	-90.6	Crn-Cam rock, coarse-grained		
DG64A	Crn-1	0.10						
DG150	Pl-1	7.30	6.1			gabbro-norite	66.44	32.614
DG150	Cpx	4.98					66.44	32.614

metamorphic rocks developed over gabbro-amphibolite on its contact with Ky-gneiss

DG153	Gt-1	2.15	1.6			Gt amphibolite on contact with gneiss	66.44	32.618
DG153	Cam	1.10						
DG-154	Gt-1	0.29	0.5			Gt amphibolite, 1.5 m from contact	66.44	32.618
DG-154	Cam-1	0.60						
DG155	Gt-1	2.14	2.6			Qz-Ky-Gt-Bi gneiss on contact with gabbro	66.44	32.618
DG155	Qz-1	4.13						
DG156	Gt	6.19	6.7			Ky-Gt-Bi gneiss, 2 m from contact	66.44	32.618

Kulezhma

metamorphic rocks developed over gabbro-norite near its contact with gneiss

Ku-3a	St-1	0.09				Cam-Ky rock with St-Pl substituting Ky		
Ku-3a	Cam	-0.28	-0.3	3.08	-74.7			
Ku-8	Crn-1	0.31	0.3			Cam-Crn rock		
Ku-8	Cam-1	0.28		2.5	-64.0			

Plotina

metamorphic rocks developed over Ky-gneiss

PL-40	Gt-1	-6.93	-6.4			Bi-Gt-Cam-Pl-rock with St-Pl substituting Ky		
PL-40	Pl	0.02						
PL-43	Gt -1	1.83	1.8			St-Gt-Cam-Pl rock, coarse-grained		
PL-43	Cam-1	1.3						

Visota 128 m

metamorphic rocks developed over amphibolitized gabbro-norite near its contact with gneiss

KV-2	Cam-1	-6.50	-6.0	2.76	-90.4	Crn-Gt-Cam rock		
<i>metamorphic rocks developed over Ky-gneiss</i>								
KV-10	Gt -1	-9.05				St-Gt-Bi-Cam rock with St-Pl developing over Ky		
KV-10	Cam-1	-7.73	-7.9	3.43	-96.4			
KV-10	Pl-1	-4.3						
KV-4	Ky-1	-14.73	-14.0	1.6	-81.5	Ky-Gt-Bi gneiss		

Pulonga

metamorphic rocks developed over amphibolites

PY-3	Ged-1	2.97	2.3			Crn-Gt-Ged rock	66.32	32.011
PY-3	Crn-1	0.67						

Peruselka

metamorphic rocks developed over amphibolites

P-11	Crn-1	0.26				Crn-Cam rock, coarse grained		
P-11	Cam	3.43	2.0	3.43	-106.7			
P-11	Pl	1.85						
P-3	Crn-1	3.45	3.5			Crn-Cam rock, coarse grained		
P-3	Cam-1	3.67			-96.0			

Sample	mineral	$\delta^{18}\text{O}$ min, ‰	$\delta^{18}\text{O}$,wr calc, ‰	H ₂ O wt% ‰	δD ‰	Rock type	Longitude	Latitude
--------	---------	---------------------------------	--------------------------------------	---------------------------	-----------------------	-----------	-----------	----------

Lyagkomina

metamorphic rocks developed over Ky-gneiss

L-1	Gt-1	-4.8	-4.3			Gt-Bi-Cam-St rock with Pl-St substituting Ky		
L-1	Cam-1	-3.05	-3.1	3.15	-69.1			

Corundum rocks outside of the Chupa Series complex

Mironova Guba

Not-15	Cam-1	-1.99				Cam-Crn rock		
Not-15	Crn	-2.34	-2.2					

Kii Island

Kii -1	Crn-1	5.04	5.5			Crn-Pl-Cam rock		
Kii-1	Cam-1	4.24		3.6	-74.7			
Kii-2	Cam-1	5.57	6.1			Crn-Pl-Cam rock		

Khetolambina, Klimovsky Rudnik

DK484	Crn-1	4.82	5.3			Crn-Cam rock		
-------	-------	------	-----	--	--	--------------	--	--

Other Belomorian metasomatic rocks

Vincha

Vch-2	Gt	11.05	11.9			Qz-Gt-St-Ky rock		
Vch-1	Qz	14.29				Qz-Gt-St-Ky rock		

Khizovara

Hiz-16	Qz	15.88	13.8			Ky quartzite with pyrite		
Hiz-16	Ky	12.96						

2.4 Ga Volcanic rocks from Karelia

TH-8	Qz	9.43				metabasalt, Elmus River, SW Karelia		
TH-8	Cpx	6.12						

Fiskenaeset Corundum deposit, Greenland

FS-1	Crn-1	5.52	6.0			leucocratic Crn-rock		
------	-------	------	-----	--	--	----------------------	--	--

Captions. See Fig. 2 for mineral abbreviations. Cam-1, Pl-1, etc means single crystal analysis.

WR $\delta^{18}\text{O}$ values were calculated using the following mineral-WR fractionation factors (see Appendix for details):

Gt-WR(mafic) = 0‰; Gt-WR(silicic) = -0.5‰; Qz-WR = 2‰; Gt=Crn=Cam; Opx=Cpx=Ged - Gt = 0.5‰; Gt-Ky = 0.25‰

Where two or more minerals were analyzed, best WR estimate is based on the above isotope fractionations and modal proportions of minerals; accuracy of such procedure is estimated at $\pm 0.5\%$; for nearly monomineralic rocks, $\delta^{18}\text{O}_{\text{rock}} = \delta^{18}\text{O}_{\text{min}}$.

If mineral is secondary or retrogressed (e.g. plagioclase, gedrite, Bi, or chlorite), WR estimate is only based on fresh refractory minerals;

Plagioclase and Bi are typically excluded from WR estimate based on their susceptibility to secondary exchange

For the lowest- $\delta^{18}\text{O}$ corundum-bearing rocks from Khitostrov, multiple $\delta^{18}\text{O}_{\text{WR}}$ estimates are given based on refractory minerals, because these rocks exhibit specimen-scale heterogeneity (Bindeman et al. 2010).

These estimates (-26.9 to -25‰), are the lowest in this dataset, and are shown with larger font.

See Bindeman et al. (Geology, 2010, electronic Table) for additional single-crystal in-depth investigation analysis of 6 more samples of Crn and Ky bearing rocks from Khitostrov for oxygen and hydrogen isotopes, which are discussed in text of this paper.

GPS Coordinates are given where measured during 2010 fieldwork; for position of other samples see Figures.

Table A2 Representative chemical analyses of silicic and mafic rocks from the Belomorian Belt and estimated of rock loss due to dissolution based on immobile element Zr (italics in %, gram element/100g of starting rock)

	<i>Khitostrov</i>				<i>Mt Dyadina</i>				<i>Varatskoye</i>						
	1 Gt-Bi gneiss	2 Ky-Gt-Bi gneiss	3 Ky-rock no Qz	4 Ky-Amph rock	5 loss (5-2) core Crn rock	6 50% model 200°C W/R=1680	7 542 Gabbro-No	8 loss (8-6) in %	9 543 Grt-amphit	10 544 Cm-St-Ky	11 53.4 Grt-Chl	12 B-51 metagab	13 B-75 Ant-Hbl(+ Crn-Hbl)	14 B-81a in %	15 loss (13-11) 69
SiO2	63.22	63.23	48.3	46.575	46.26	-62 45	51.17	53.16	38.84	-65	37.47	45.80	45.80	33.90	-77
TiO2	0.53	0.66	1.13	1.27	1.16	-8 1	0.54	0.71	1.43	23	0.85	0.60	0.75	1.60	-17
Al2O3	15.22	16.83	21.9	22.2	24.09	-25 28	13.85	14.65	28.06	-6	22.50	11.50	12.25	25.30	-32
Fe2O3	3.76	0.92	1.55	1	1.79	1 6.1	10.23	9.94	9.11	-59	16.58	3.27	1.45	3.55	-66
FeO	4.55	5.9	8.69	11.165	10.12	-10 5.1					0.00	8.58	10.30	9.10	-67
MnO	0.06	0.08	0.03	0.14	0.07	-54	0.156	0.166	0.115	-66	0.21	0.15	0.16	0.22	-55
MgO	3.16	3.67	5.05	6.12	6.01	-15 6	11.71	9.48	7.00	-72	17.61	15.80	16.43	9.47	-81
CaO	2.38	2.13	2.57	5.24	4.74	16 3.8	7.97	7.55	13.08	-24	4.61	9.45	7.26	10.95	-64
Na2O	3.44	2.62	4.8	3.785	4.62	-8 1.2	2.33	2.51	0.65	-87	0.61	1.86	1.75	2.18	-64
K2O	2.34	2.18	3.97	1.215	0.53	-87 2.8	0.91	0.77	0.38	-81	0.27	0.20	0.16	0.32	-50
H2O-	0.20	0.23	1.94								0.01	0.28	0.2	0.15	-83
LOI	0.85	1.26									0.00	1.76	2.22	2.15	-62
P2O5							0.99	0.86	1.24		0.00	0.07	0.13	0.16	-29
CO2							0.10	0.14	0.04	-81	0.14	0.29	0.23	0.35	-63
Sum	99.71	98.22	97.99	98.71	99.39	99.0	99.96	99.94	99.95		100.85	99.61	99.09	99.40	
Li	67	53					0.04	0.05	0.05	-42					
Rb	101	89			15	-91	28	18	6	-90		2	4	7	9
Cs	4	7			0.55	-96									
Sr	366	219			485	15	256	313	727	32		9	33	582	1905
Ba	570	420			139	-83	322	338	32	-95		36	44	45	-61
Sc	16				18		27	33	27	-53		33	34	56	-47
V	150	178			152	-56	170	162	174	-52		126	144	263	-35
Cr	180	304			303	-48	801	542	344	-80		1220	1602	559	-86
Co	29	38					57	55	19	-84		62	76	62	-69
Ni	120	156			178	-41	249	199	133	-75		486	528	322	-79
Cu	55	79			2	-99	55	72	10	-92		23	44	27	-64
Zn	104	111			29	-86	86	85	57	-69		115	110	79	-79
Ga	18	24			32	-30	14	14	29	-3					
Y	14	23			15	-66	17	19	22	-40		17	22	40	-27
Zr	101	99			190		76	103	163			63	96	203	
Pb	14	5.5			14	33	7	3	19	26		0	1	14	
La	25	22			46	9	12.76	13.86	17.27	-37		6.2	7.41	40.01	100
Ce	50	43.5			108	30	26.07	28.63	37.87	-32		19	20.15	90	47
Pr							3.12	3.6	4.79	-28		2.56	2.72	10.89	32
Nd	27	24			44	-4	13.12	13.67	17.94	-36		10.38	12.74	42.57	27
Sm	4.9	4.5			7	-16	1.9	1.93	2.94	-28		2.47	2.6	7.7	-3
Eu	1.3	1.1			1.4	-33	0.81	0.7	0.87	-50		0.67	0.67	1.47	-32
Gd	3	3.35			4.7	-28	2.58	2.71	3.42	-38		2.58	3.61	8.34	0
Dy							2.37	2.14	3.22	-37		2.08	3.15	7.05	5
Er	1.2	1.65			1.4	-56	1.11	1.1	1.93	-19		1.32	2.47	3.7	-13
Tb							0.4	0.38	0.52	-39		0.42	0.59	1.22	-10
Yb	0.7	1.3			1.2	-52	1.17	0.92	1.97	-22		1.24	2.62	3.83	-4
Lu					0.18		0.21	0.21	0.28	-38		0.18	0.5	0.68	17
Hf					5.2										
Nb					8.4		2	5	16	273		4	3	11	-15
Th					16.1										
U					1.4										
Ta					0.53										
Cl							861	1288	109	-94					

Caption: analyses 1 and 2 are averages from: Ruchyev A.M. (2002) Trace and noble metals in gneisses of Chupa suite (Belomorian complex, northern Karelia. in book: Geology and ore deposits of Karelia, vol. 5, Petrozavodsk, 49p. analysis 5 is average of K1 and K2 rocks from Bindeman et al. (Geology, 2010); analyses 3,4 are from Serebryakov (2004); others are unpublished analyses
Model: gneiss 1 dissolution experiment in Chiller program using fresh water at 200 C

Table A2 Compilation of isotope fractionation factors to estimate whole-rock value based on minerals

To estimate WR values the following isotope fractionations were used:

WR-Gt mafic	0
WR-Gt silicic	0.5
WR-Qz	-2

Calculations below demonstrate validity of this.

Mineral pair	T, °C	$\Delta 18\text{O}$ Reference
Qz-An70	600	2.2 Chiba et al. 1988
Qz-An40	600	1.65 Chiba et al. 1989
Qz-Ab	600	1.23 Chiba et al. 1989
Qz-An	600	2.61 Chiba et al. 1989
Qz-Ged	600	3.7 Zheng, 1993
Qz-Ky	600	2.26 Zheng, 1993
Qz-Phengite	600	2.38 Zheng, 1993
Qz-Bi	600	3.74 Zheng, 1993
Qz-Hb	600	2.39 Kohn and Valley 1998
Qz-Gt, Ca-pool	600	2.01 Kohn and Valley 1998
Qz-corundum	600	2.01 Polyakov and Ustinov, 1997
Qz-Rutile	600	5.97 Chacko et al. 1996
Qz-Magnesite	600	0.5 Clayton et al. 1989
Qz-Zoisite	600	2.05 Matthews et al. 1993
Qz-Chlorite	600	3.08 Zheng 1993

Relative to garnet:

		$\Delta 18\text{O}$
		Gt-min
Gt-Qz	600	-2.39
Gt-An70	600	0.2
Gt-An40	600	-0.35
Gt-Ab	600	-0.77
Gt-An	600	0.61
Gt-Ged	600	1.7
Gt-Ky	600	0.26
Gt-Phengite	600	0.38
Gt-Bi	600	1.74
Gt-Hb	600	0.39
Gt-Gt	600	0.0
Gt-ruby	600	0.0
Gt-rutile	600	3.97
Gt-Magnesite	600	-1.5
Gt-Epidote	600	0.05
Gt-Chlorite	600	1.08

Examples of estimations:

Rock:	modal %	Gt-WR fractionation
mafic lithology		
Gt	0.17	
Amph	0.15	
Plag, An40	0.45	
Bi	0.12	
Ky	0.05	
Qz	0.05	
Sum	0.99	0.00
silicic lithology		
Gt	0.1	
Amph	0.05	
Plag, An40	0.5	
Bi	0.12	
Qz	0.23	
Sum	1	-0.50

Chacko, T., Hu, X.S., Mayeda, T.K., Clayton, R.N. & Goldsmith, J.R. (1996). Oxygen isotope fractionations in muscovite, phlogopite, and rutile, *Geochimica et Cosmochimica Acta* 60: pp. 2595-2608.

Chiba H., Chacko T., Clayton R.N. & Goldsmith J.R. (1989) Oxygen isotope fractionations involving diopside, forsterite, magnetite, and calcite: Applications to geothermometry. *Geochim Cosmochim Acta*, 53, p. 2985-2995.

Kohn, MJ and Valley, JW (1998). Effects of cation substitutions in garnet and pyroxene on equilibrium oxygen isotope fractionations. *J. Metamorphic Geol.*, 16, 625-639.

Matthews, A., Goldsmith, J.R. and Clayton, R.N. (1983). Oxygen isotope fractionation between zoisite and water. *Geochim. Cosmochim. Acta* 47, pp. 645-654.

Polyakov, V.B., Ustinov, V.I., 1997. Isotope equilibrium constants (b O-18 factors) of corundum. *Geochem Int.* 10, 1019-1025.

Zheng, Y.-F. (1993). Calculation of oxygen isotope fractionation in hydroxyl-bearing silicates. *Earth Planet. Sci. Lett.* 120, pp. 247-263.

Figures for the electronic supplementary material

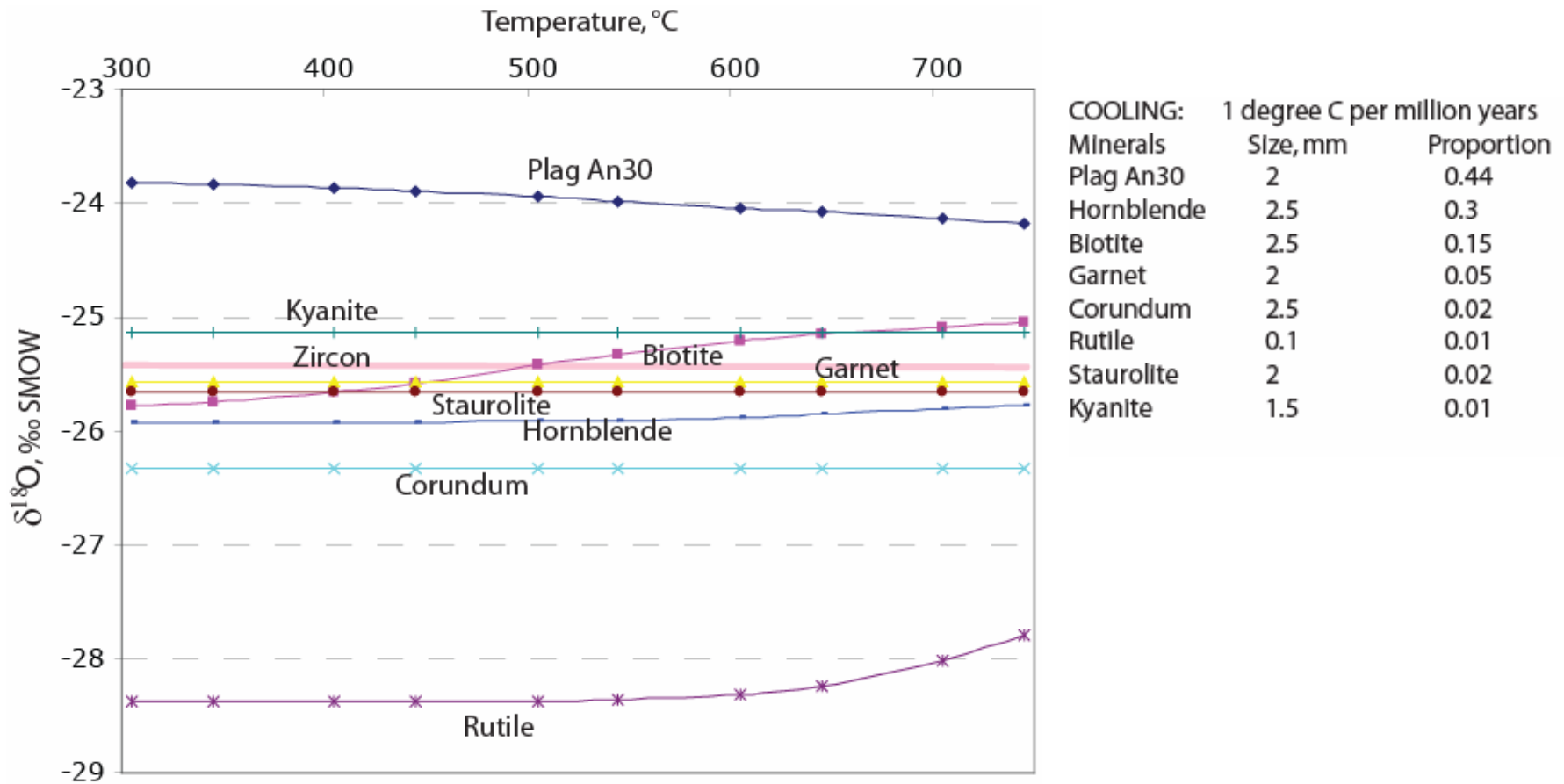


Fig. A1 Retrogression of oxygen isotopic values in a typical corundum bearing assemblage as a function of cooling and differential closure using Fast Grain Boundary diffusion model of Eiler, Baumgartner, and Valley, (1993). Notice that even at slow cooling rate of 1 degree per million years corundum, garnet, hornblende, staurolite, and kyanite do not retrogress and preserve their original, peak metamorphic temperature of formation. Plagioclase, rutile, and biotite display retrogression of less than 0.7 permil. Sizes of minerals and their proportions are given in the table. At faster cooling rate even less retrogression is expected. Therefore, Isotope heterogeneity observed within hand specimen (see Table A1 and Bindeman et al. 2010, Fig. 2) cannot be explained by differential retrogression and must reflect source variability and interaction with external fluids.

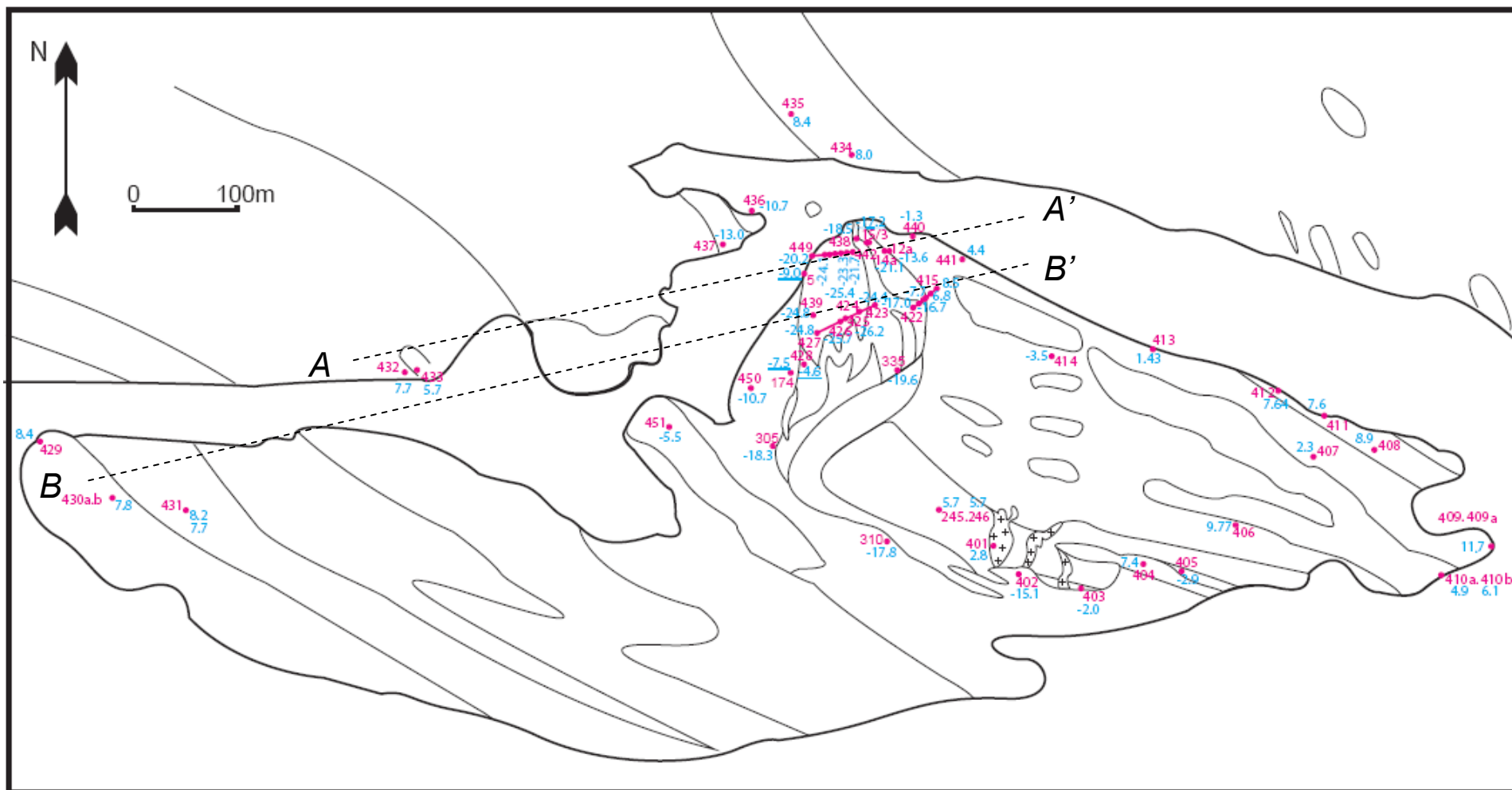


Fig. A2 Sampling map of Khitostrov locality with sample names shown in red, and oxygen isotopic values shown in blue. Location of two profiles are shown by dashed lines (Figs. 4a,b in the text). See Fig. 2 in the text for geological map.

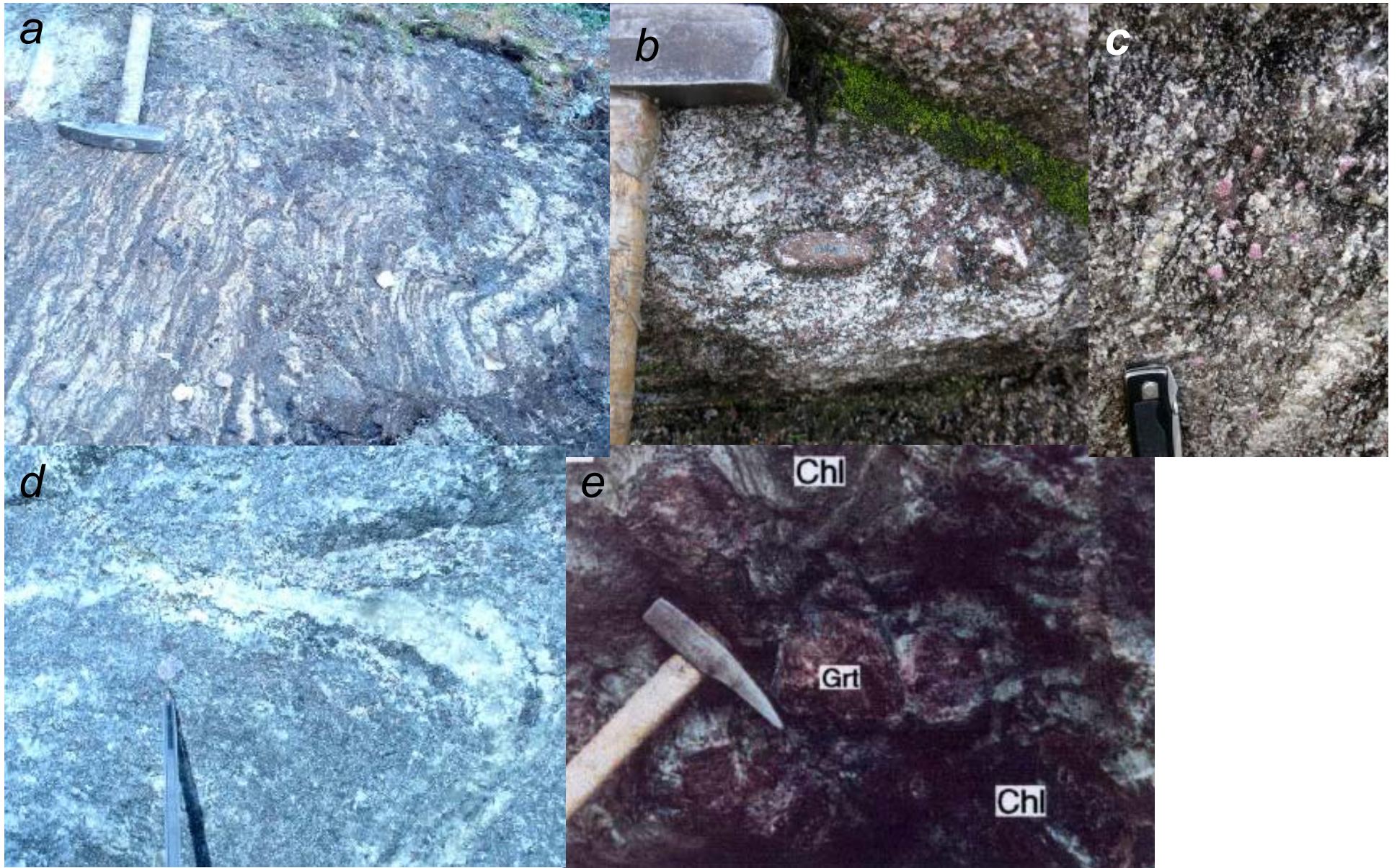


Fig. A3 Field relations between different rock types: a) original Chupa gneiss; b) St-Pl pseudomorphs over large crystal of Ky at Khitostrov; c) rock with large Crn; d) Corundum-bearing rock (pen is pointing to Crn), impregnated by plagioclazite at Khitostrov; e) large crystals of garnet in chloritic rock inside amphibolite at Mt. Dyadina.

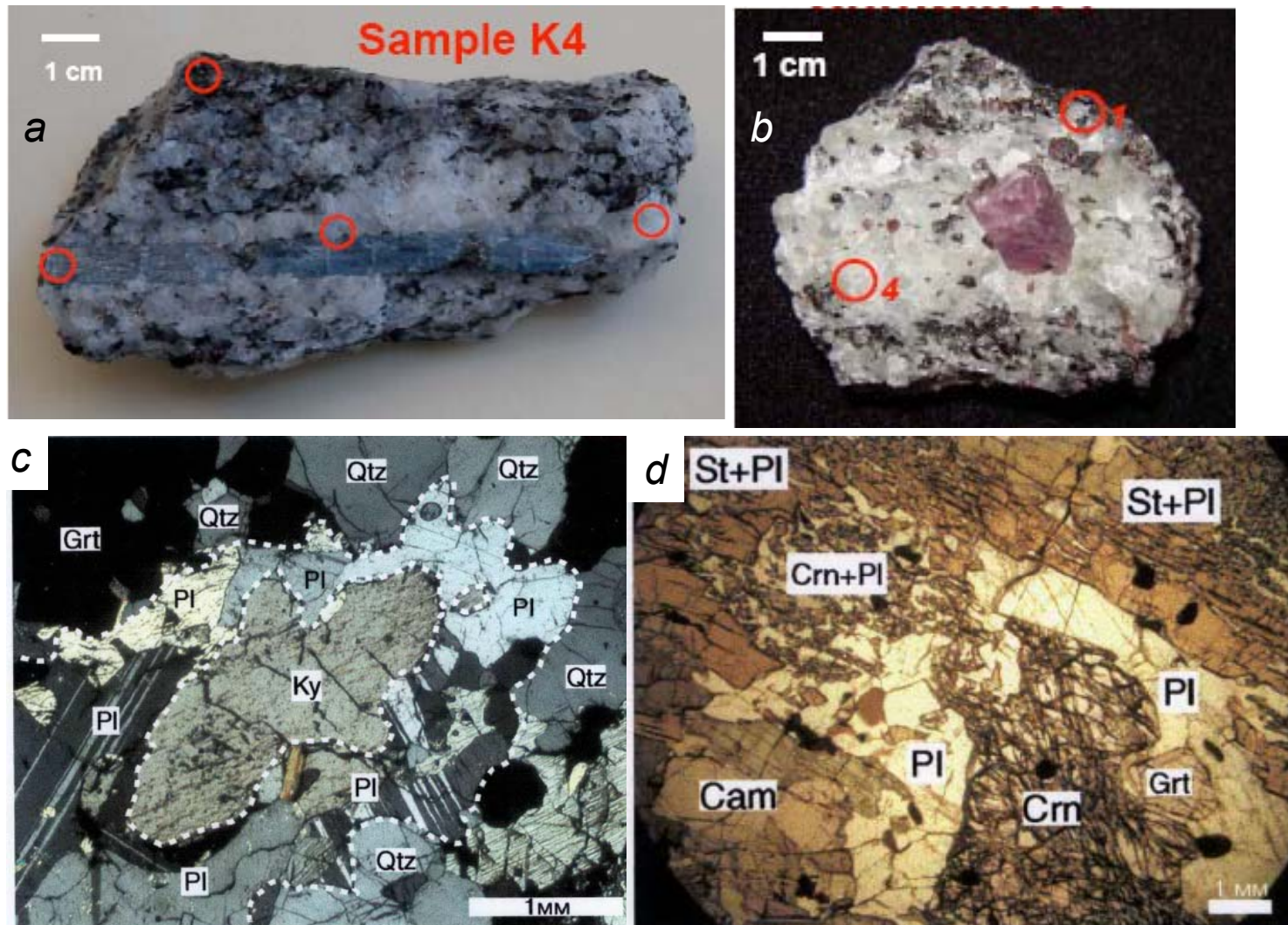


Fig. A4 Hand specimen and thin sections showing different rock types. a-b) kyanite and corundum from Khitostrov with indicated areas sampled by crystal-cluster isotope analysis (sample K4 and K1 of Bindeman et al. 2010); c) thin sections showing reactive relationship between kyanite and Qtz (Varatskoye) and d) Crn-St-Pl symplectite over Ky, with large corundum appearing inside (Khitostrov).